

NIED Seismic Moment Tensor Catalogue January – December 1998

By

Eiichi Fukuyama*, Mizuho Ishida*, Shigeki Horiuchi*, Hiroshi Inoue*,
Sadaki Hori*, Shoji Sekiguchi*, Hiroyuki Kawai[†], and Hiroshi Murakami[‡]

*National Research Institute for Earth Science and Disaster Prevention

[†]Sun Microsystems K.K.

[‡] Earthquake Observation Research Technology Center

Abstract

We have routinely estimated the moment tensors of earthquakes occurring in and around Japanese islands. This report compiles all the moment tensor solutions we have estimated in 1998. In these computations, we used the FREESIA/KIBAN broadband seismic network developed by NIED (National Research Institute for Earth Science and Disaster Prevention) and STA (Science and Technology Agency). We mainly used STS-1 broadband seismometer records. VSE311 (now upgrading to VSE355) strong motion velocity-meter was additionally used in cases when STS-1 waveforms were unavailable. Moment tensor estimation is triggered by the JMA (Japan Meteorological Agency) e-mail of emergent hypocenter location information. This catalogue includes most $M > 4.0$ earthquakes and some $M > 3.5$ earthquakes. However, due to either incomplete station distribution or the quality of available data, our catalog missed several earthquakes that had been detected by JMA.

Key words: Seismic moment tensor, Earthquake catalogue

1. Method

Below is a brief description of the method used here to determine seismic moment tensors and their centroid depths. Fukuyama et al. (1998) describes the method and it would be helpful to refer to this in more details. All the informations concerning this catalogue are also displayed at the World Wide Web page¹.

Moment tensor analysis is triggered by the JMA (Japan Meteorological Agency) emergency hypocenter report received by e-mail. The following information is used from the report: origin time (in minutes), epicentral location (in 0.1 degree), depth (in 10km) and magnitude. This e-mail is dispatched for earthquakes with a maximum JMA scale intensity

¹<http://argent.geo.bosai.go.jp>

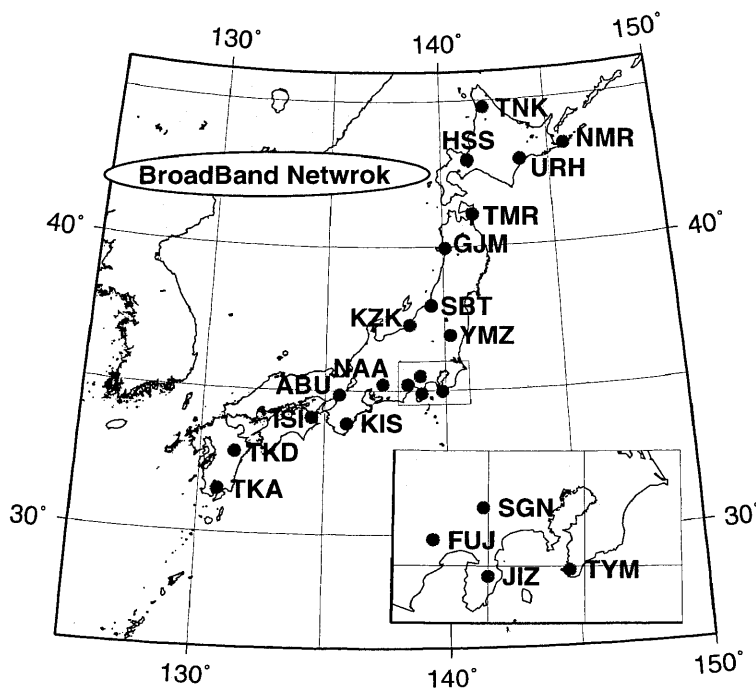


Fig. 1 Broadband station distribution used in the analysis.

greater than 1 in the Kanto-Shinetsu-Chubu region (central part of Japan) and its surroundings. For other regions, the e-mail is dispatched only for earthquakes with a maximum intensity 3 or more. This information covers most $M > 3.5$ earthquakes. However, it sometimes misses off shore or deep $M > 3.5$ earthquakes, thus we used the information from the JWA (Japan Weather Association) World Wide Web page² as a supplement.

All the stations used in this analysis are shown in Fig. 1 and Table 1. Three stations at most are used for the moment tensor estimation. Filter coefficients and minimum epicentral distance are chosen according to the JMA magnitude (see Table 2). The JMA magnitude is used only for this purpose. The criterion for choosing stations is basically on its epicentral distance. The closest three stations within the epicentral distance range are chosen as a first (automatic) trial. We then update it manually by examining station combinations, adjusting origin time offsets, or adjusting source depth. This is because if the waveforms are contaminated by long period noise, the solution is no more reliable. Manual operation is mainly to remove these noisy records. If the dataset is well examined, the moment tensor solution can be determined stably and uniquely by adjusting origin time offset and its source depth. In this catalogue, all solutions have been inspected and re-computed as final solutions.

Filtered displacement waveforms are used for the moment tensor inversion. The filter coefficients vary according to JMA magnitude (Table 2). 1 Hz sampling displacement data produced from the original 20Hz data stream (VBB components) are used in order to reduce the latency caused by packeting during the transmission from each station.

The moment tensor estimation consists of two steps, an automatic process and a manual

²<http://tenki.or.jp/quake.html>

Table 1 Locations of stations used in the analysis.

Station Name	Station Code	Latitude ($^{\circ}N$)	Longitude ($^{\circ}E$)	Height (m)	Cooperative Organization	Funding Project
Abuyama	ABU	34.8603	135.5734	138	Kyoto U.	KIBAN
Fujigawa	FUJ	35.2267	138.4217	640	Tokyo U.	FREESIA
Gojyome	GJM	39.9517	140.1167	105	Tohoku U.	KIBAN
Sapporo	HSS	42.9647	141.2328	230	Hokkaido U.	FREESIA
Tokushima	ISI	34.0572	134.4580	27	Kyoto U.	FREESIA
Nakaizu	JIZ	34.9129	138.9972	263	—	FREESIA
Kiwa	KIS	33.8627	135.8933	70	Kyoto U.	FREESIA
Kashiwazaki	KZK	37.2951	138.5156	220	Tokyo U.	FREESIA
Asahi	NAA	35.2217	137.3650	200	Nagoya U.	FREESIA
Nemuro	NMR	43.3650	145.7430	20	Hokkaido U.	FREESIA
Shibata	SBT	37.9656	139.4538	160	Tohoku U.	KIBAN
TsuruSugeno	SGN	35.5054	138.9475	800	—	FREESIA
Takakuma	TKA	31.5125	130.7853	535	Kagoshima U.	FREESIA
Takeda	TKD	32.8140	131.3900	751	Kyushu U.	FREESIA
Tomari	TMR	41.0990	141.3868	120	Hirosaki U.	KIBAN
Nakagawa	TNK	44.7757	142.0830	60	Hokkaido U.	FREESIA
Tateyama	TYM	34.9708	139.8481	30	Geogr. Surv. Jpn.	FREESIA
Urahoro	URH	42.9270	143.6746	75	Hokkaido U.	KIBAN
Yamizo	YMZ	36.9241	140.2479	555	Tohoku U.	KIBAN

one with human inspections. In the automatic stage, by using JMA e-mail, three stations are chosen automatically to prepare the waveform dataset. Using these waveforms, a moment tensor inversion is conducted with several trial depths within ± 30 km from the JMA hypocenter depth. Assumed depth points are shown in Table 3. In the manual determination stage, the combination of stations, optimum zero offset and depth have been examined by the operator in a Monte Carlo manner. At this point, the error function is set to variance reduction (*VarRed*) defined as follows:

$$VarRed = 100 \times \sum_i w_i \int \left(1 - \frac{(s_i(t) - o_i(t))^2}{|s_i(t)||o_i(t)|} \right) dt \quad [\%] \quad (1)$$

where $s_i(t)$ and $o_i(t)$ are synthetic and observed waveforms respectively. w_i is a weighting function proportional to the hypocentral distance.

The velocity structure used for Green's function is shown in Table 4. This structure is constructed by referring to Ukawa et al. (1984) for the shallower part and Fukao (1977) for the deeper part. Green's function is computed by using the discrete wavenumber method developed by Saikia (1994). The program named *tdmt_inv* is used for the moment tensor estimation which is developed by Pasyanos et al. (1996). *tdmt_sched.pl* is a Perl script developed here and used in the routine process. *tdmt_sched.pl* controls the automatic procedure. *tdmt_manual.pl* then supports the human inspection of the automatic moment tensor solution by referring to the automatic solution. In this inversion, since the time offset is shifted either automatically or manually, the centroid location is not estimated. This offset

Table 2 Minimum epicentral distance, filter coefficients, and data length for initial magnitude reported by JMA

Magnitude range	Epicentral Dist. (<i>km</i>)	Frequency range (<i>Hz</i>)	Data length (<i>seconds</i>)
3.5 <M <5.0	>50	0.02 – 0.05	120
5.0 <M <6.5	>100	0.01 – 0.05	120
6.5 <M <7.5	>300	0.01 – 0.05	150
7.5 <M	>600	0.005 – 0.02	180

Table 3 Assumed source depths in km used in the analysis.

5	8	11	14	17	20	23	26	29	32	35	38	41	44	47	50	53	56	59	62	65	68	
71	74	77	80	83	86	89	92	95	98	101	104	107	110	113	116	119	122					
125	130	135	140	145	150	155	160	165	170	175	180	185	190	195	200							
210	220	230	240	250	260	270	280	290	300	320	340	360	380	400								

adjustment corrects both velocity structure misfit and centroid location misfit. As shown in Fukuyama et al. (1998), the shape of Green’s function does not change for slight epicentral distance change, so that the above procedure works.

2. Results

The results are shown in Table 4, Figs. 2 and 3. In Table 3, origin times, latitudes, longitudes and region names are provided by JMA e-mail. Other parameters such as D (depth), Mw (moment magnitude) etc., are determined by this analysis. VarRed represents variance

Table 4 Velocity structure for Green’s functions.

Depth (<i>km</i>)	Thickness (<i>km</i>)	P Velocity (<i>km/s</i>)	S Velocity (<i>km/s</i>)	Density (<i>kg/m³</i>)	Q_P	Q_S
0	3	5.50	3.14	2300	600	300
3	15	6.00	3.55	2400	600	300
18	15	6.70	3.83	2800	600	300
33	67	7.80	4.46	3200	600	300
100	125	8.00	4.57	3300	600	300
225	100	8.40	4.80	3400	600	300
325	100	8.60	4.91	3500	600	300
425	–	9.30	5.31	3700	600	300

reduction, showing as percentages. (Str1, Dip1, Rak1) and (Str2, Dip2, Rak2) are two fault planes. Str, Dip, and Rak indicate strike, dip and rake angles, respectively. M_{xx} , M_{xy} , M_{xz} , M_{yy} , M_{yz} , and M_{zz} are the moment tensor components normalized by M_o (total scalar moment). In Fig. 2, the best fit double couples are shown with their epicentral locations. The numerals appearing above each focal mechanism represent the event ID shown in Table 5. In Fig 3, moment tensors are shown with lower hemisphere projection. P- and T- axes are also shown. Superscripted numerals again indicate event ID.

3. Conclusion

We have estimated 284 seismic moment tensors and their centroid depths by using FREESIA /KIBAN broadband waveforms.

Acknowledgments

The FREESIA broadband seismic network is supported by the NIED project entitled ‘Fundamental Research on Earthquakes and the Earth’s Interior Anomaly’ under the cooperation of Hokkaido University, Tokyo University, Nagoya University, Kyoto University, Kyushu University, Kagoshima University, and the Geographical Survey of Japan. The KIBAN broadband seismic network is supported by the Science and Technology Agency under the cooperation of the Earthquake Research Council.

References

- 1) Fukao, Y. (1977): Upper mantle P structure on the ocean side of the Japan–Kurile Arc, *Geophys. J. Roy. astr. Soc.*, **50**, 621-642.
- 2) Fukuyama, E., M. Ishida, D. S. Dreger and H. Kawai (1998): Automated seismic moment tensor determination by using on-line broadband seismic waveforms, *Zisin*, **51**, 149-156 (in Japanese with English abstract).
- 3) Pasyanos, M. E., D. S. Dreger and B. Romanowicz (1996): Toward real-time estimation of regional moment tensors, *Bull. Seismol. Soc. Am.*, **86**, 1255-1269.
- 4) Saikia, C. K. (1994): Modified frequency-wavenumber algorithm for regional seismograms using Filon’s quadrature: modelling of Lg wave in eastern North America, *Geophys. J. Int.*, **118**, 142-158.
- 5) Ukawa, M., M. Ishida, S. Matsumura and K. kasahara (1984): Hypocenter determination method of the Kanto-Tokai observational network for microearthquakes, *Research Notes of the National Research Center for Disaster Prevention*, **53**, 1-88 (in Japanese with English abstract).

NIED 地震モーメントテンソルカタログ

1998年1月－12月

福山英一*・石田瑞穂*・堀内茂木*・井上公*・
堀貞喜*・関口渉次*・川井啓廉†・村上寛‡

要旨

我々は、日本及びその周辺で発生する地震のモーメントテンソルを定常的に決めている。このレポートは、1998年に決められたすべての地震のモーメントテンソル解をコンパイルしたものである。防災科学技術研究所及び科学技術庁により整備された広帯域地震観測網のデータを用いて計算を行った。解析には主に STS-1 型広帯域地震計の波形を用いたが、利用できない場合は、VSE311 型速度型強震計 (一部はその後継機種 VSE355 型に置き換えられている) を用いた。気象庁から発信される緊急震源情報を含んだ電子メールにより解析を開始させた。本カタログは、ほとんどのマグニチュード 4 以上の地震といくつかのマグニチュード 3.5 以上の地震をカバーしている。しかしながら、観測点分布の偏りや、波形データのノイズ状況により、気象庁により検知された地震のいくつかは解が決まらず、カタログからは洩れている。

キーワード：モーメントテンソル, 地震カタログ

*防災科学技術研究所

†サン・マイクロシステムズ株式会社

‡有限会社 地震観測技術センター

Table 5 Estimated moment tensors (continued).

Table with columns: No., Origination Time (UT), Lat (N), Lon (E), D (km), Mw, Mg (N/m), Var/Rec, Region name, Str, Dip1, Rak1, Str2, Dip2, Rak2, Mxx, Mxy, Mxz, Myy, Myz, Mzz, used Stations. Rows include seismic events from 1998/04/23 to 1998/06/21.

Table 5 Estimated moment tensors (continued).

No.	Origin Time(UT)	Lat(N)	Lon(E)	D(km)	Mw	Mo(Nm)	VarRed	Region name	Str1	Dip1	RaK1	Str2	Dip2	RaK2	Mxx	Mxy	Mxz	Myy	Myz	Mzz	used Stations
281	1998/12/19,02:09	35.5	139.0	23	3.7	3.78e14	73.83	eastern Yamanashi pref	228	48	87	53	42	83	-0.5894	0.5194	-0.0465	-0.3861	0.0840	0.9735	FUJ
282	1998/12/22,10:23	36.1	140.6	50	4.3	2.70e15	77.27	southern Ibaraki pref	330	63	-41	81	54	-146	0.7075	0.5496	-0.1085	-0.1871	0.5295	-0.5204	YMZ TYM SGN
283	1998/12/24,19:08	32.0	131.9	65	4.3	2.95e15	70.72	Hyuganada region	49	75	65	290	29	147	-0.6862	0.2329	0.5459	0.2494	-0.5395	0.4368	TKD ISI
284	1998/12/25,10:39	37.4	139.4	5	3.8	6.38e14	87.61	western Fukushima pref	65	87	153	157	63	4	0.5958	0.6066	0.4077	-0.7083	-0.1919	0.1125	SBT KZK YMZ

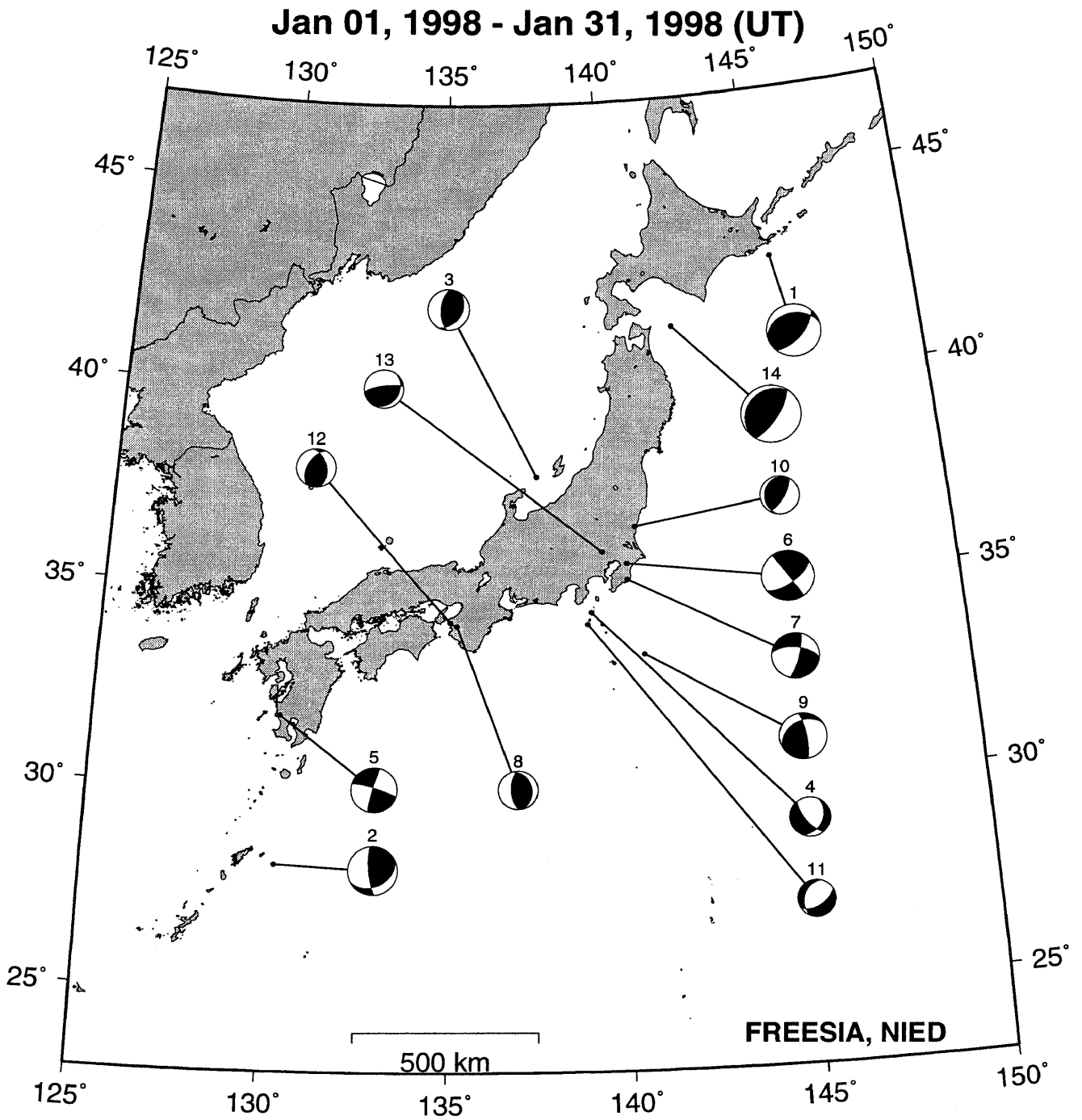


Fig. 2 Estimated focal mechanisms plotted with epicentral locations.

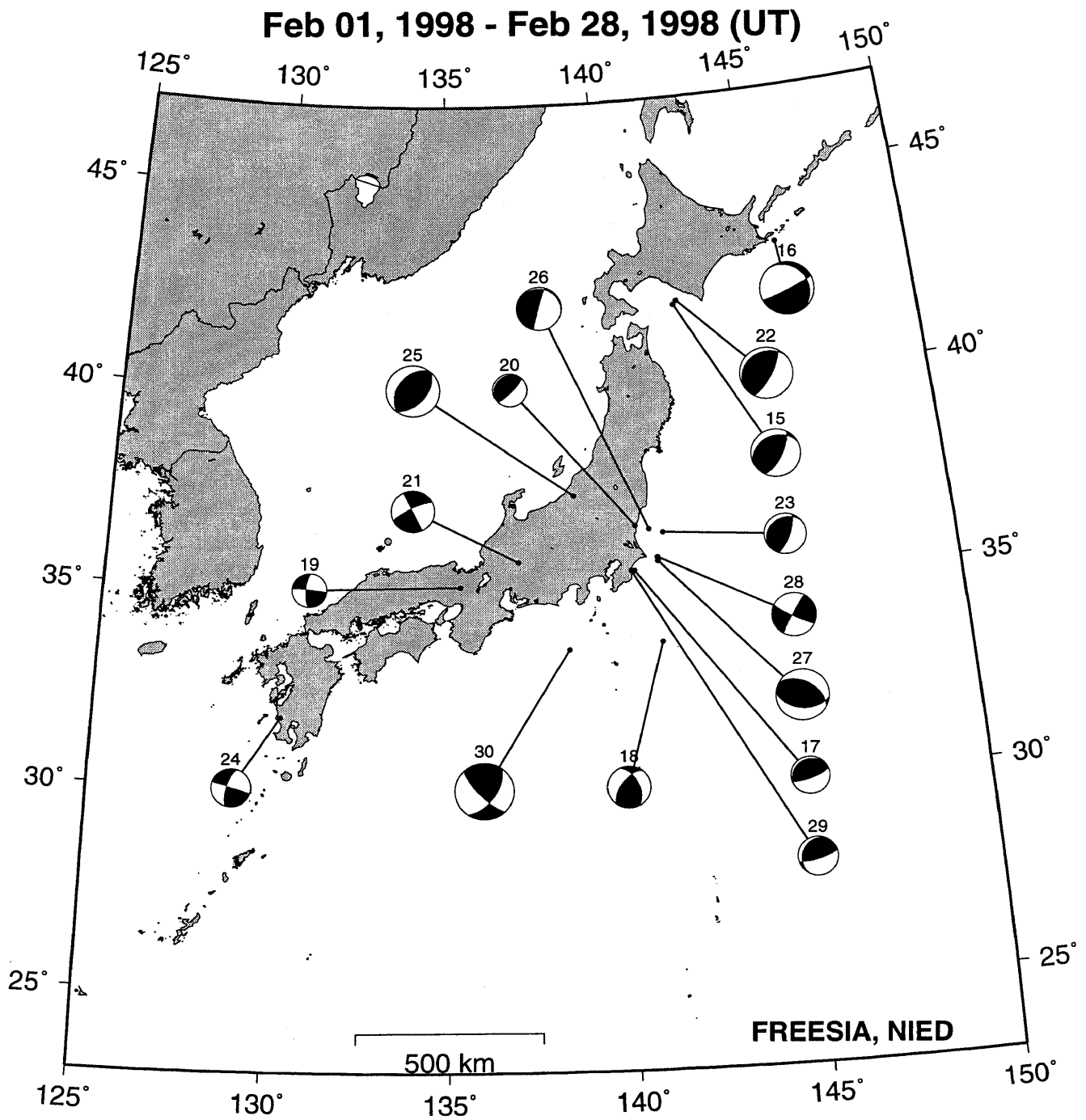


Fig. 2 Estimated focal mechanisms plotted with epicentral locations (continued).

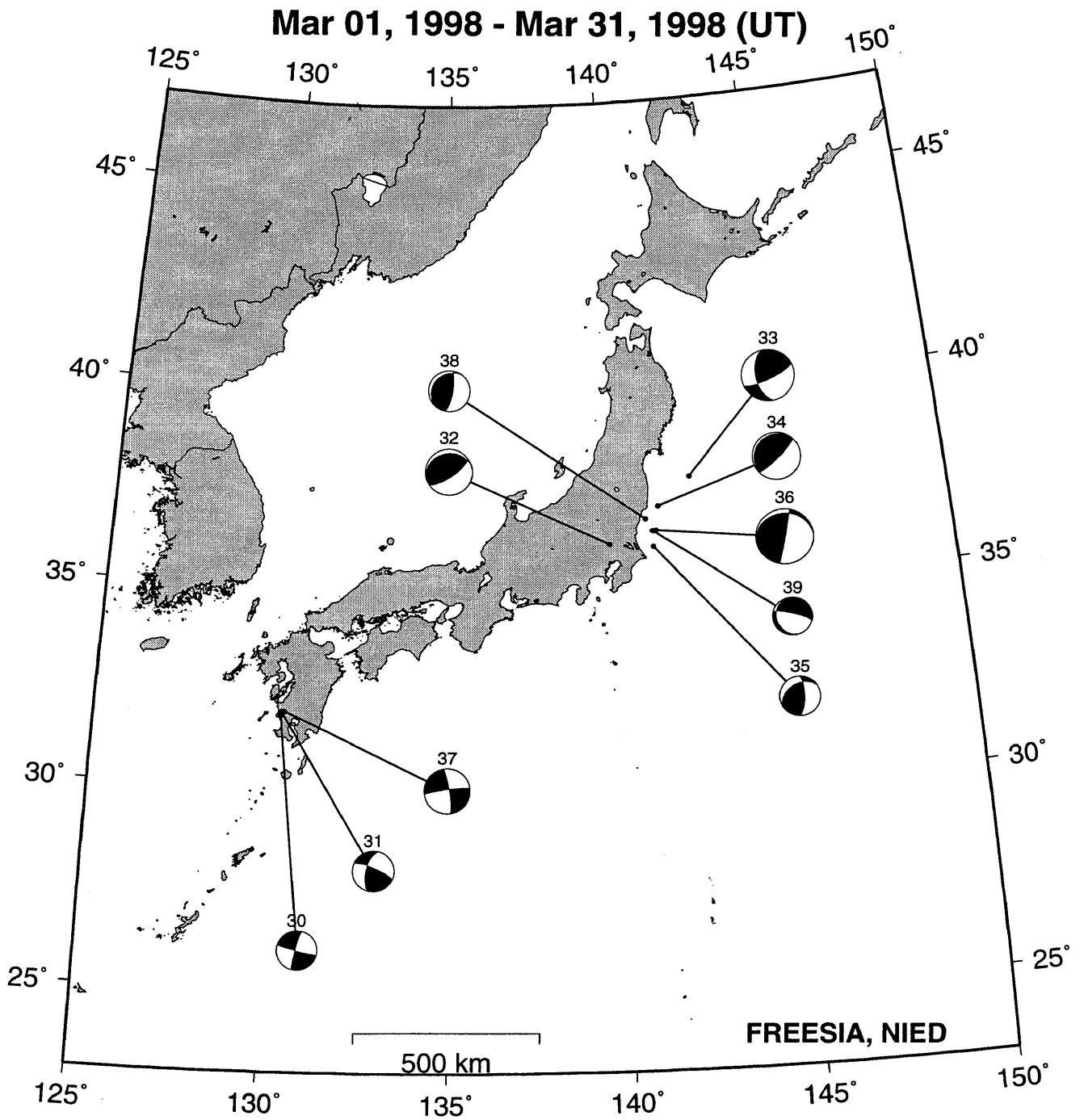


Fig. 2 Estimated focal mechanisms plotted with epicentral locations (continued).

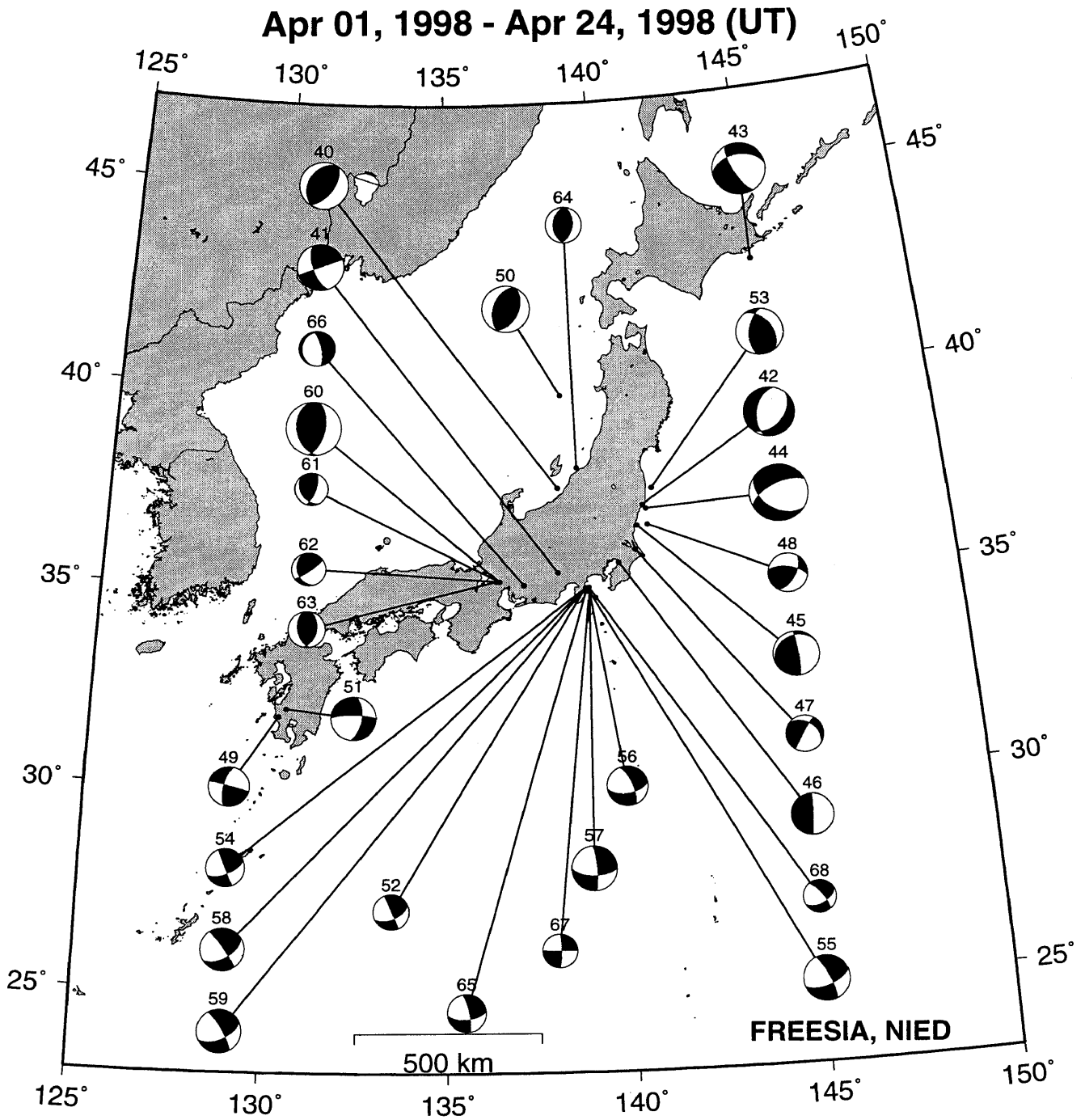


Fig. 2 Estimated focal mechanisms plotted with epicentral locations (continued).

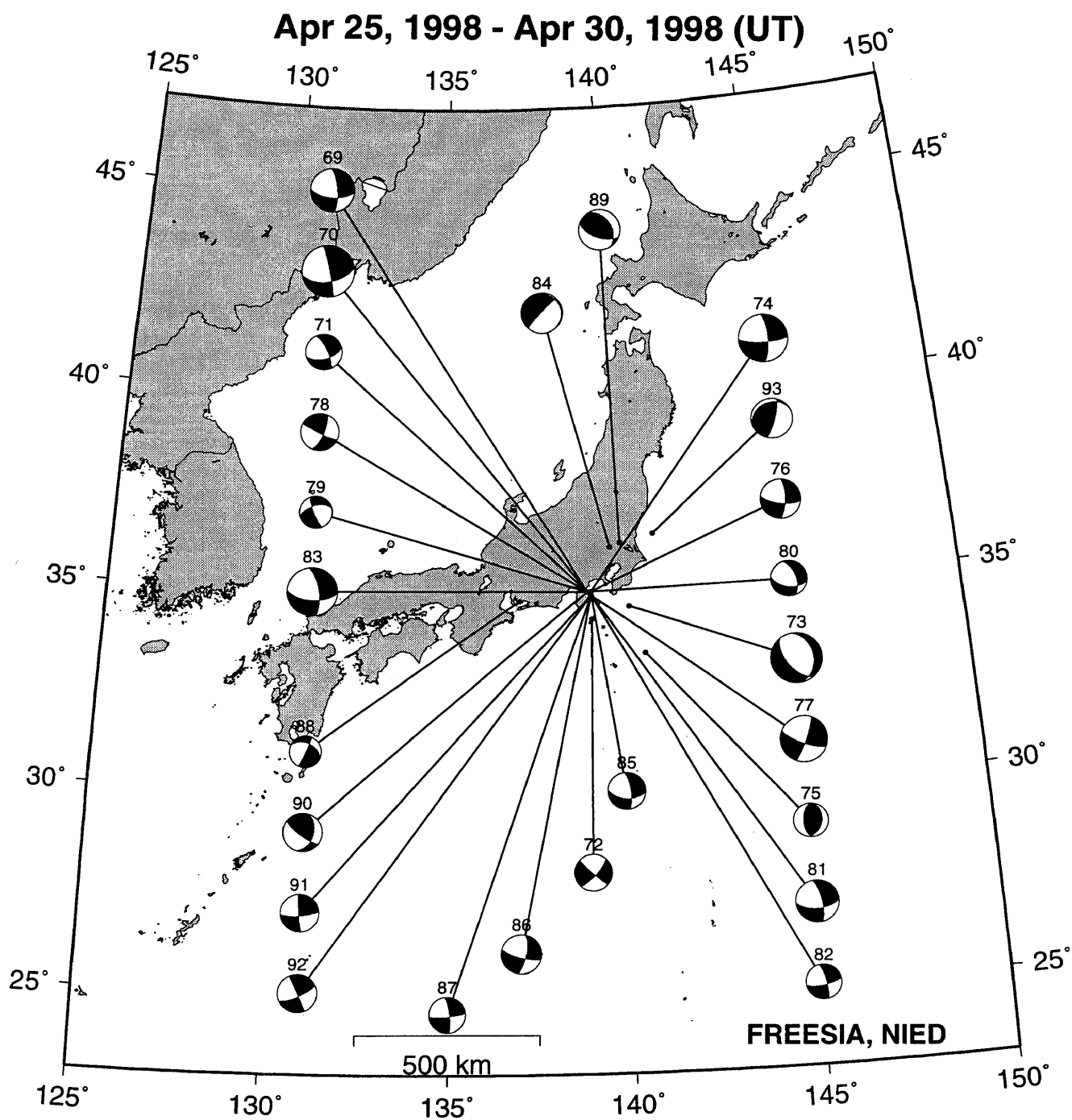


Fig. 2 Estimated focal mechanisms plotted with epicentral locations (continued).

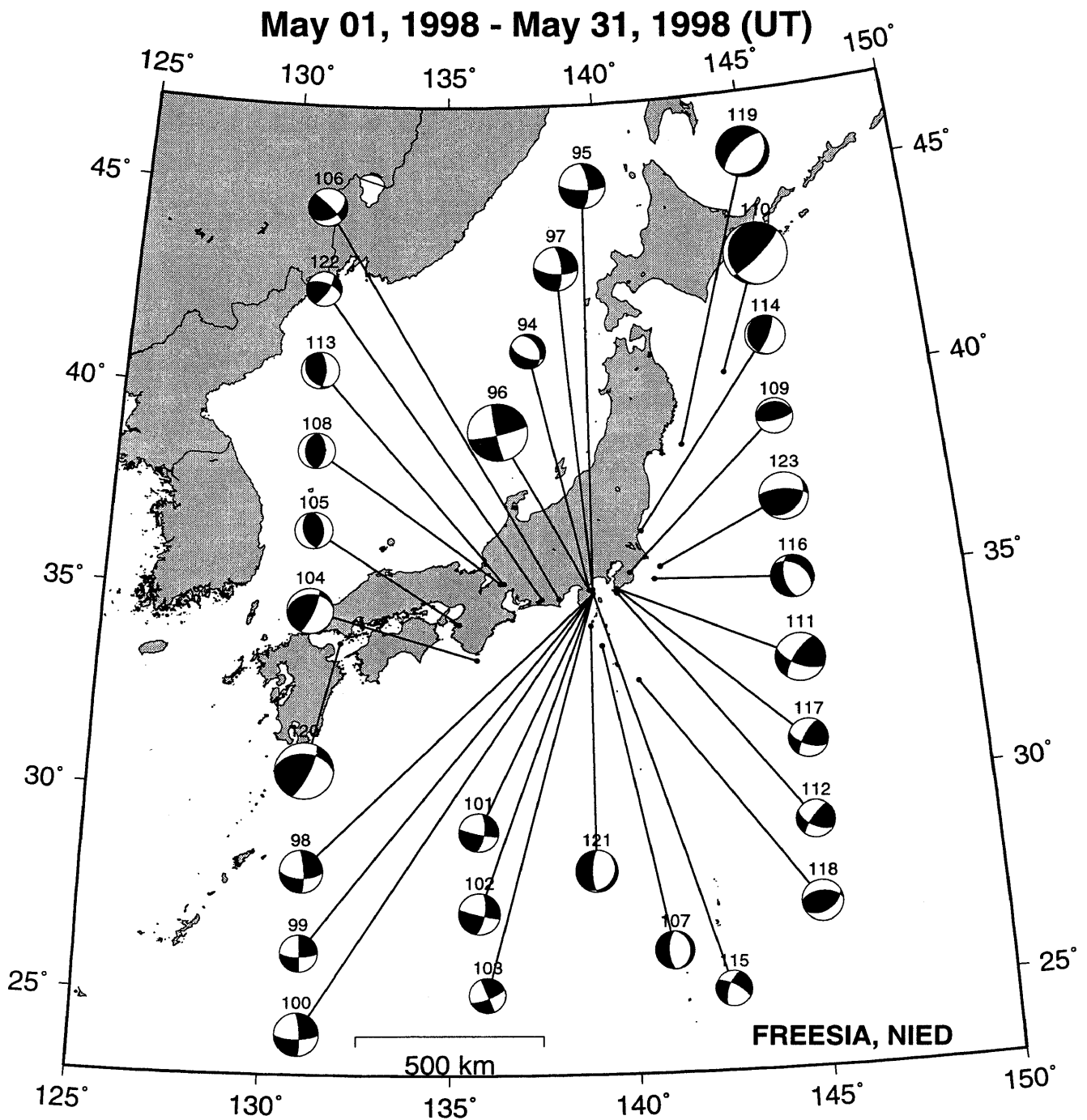


Fig. 2 Estimated focal mechanisms plotted with epicentral locations (continued).

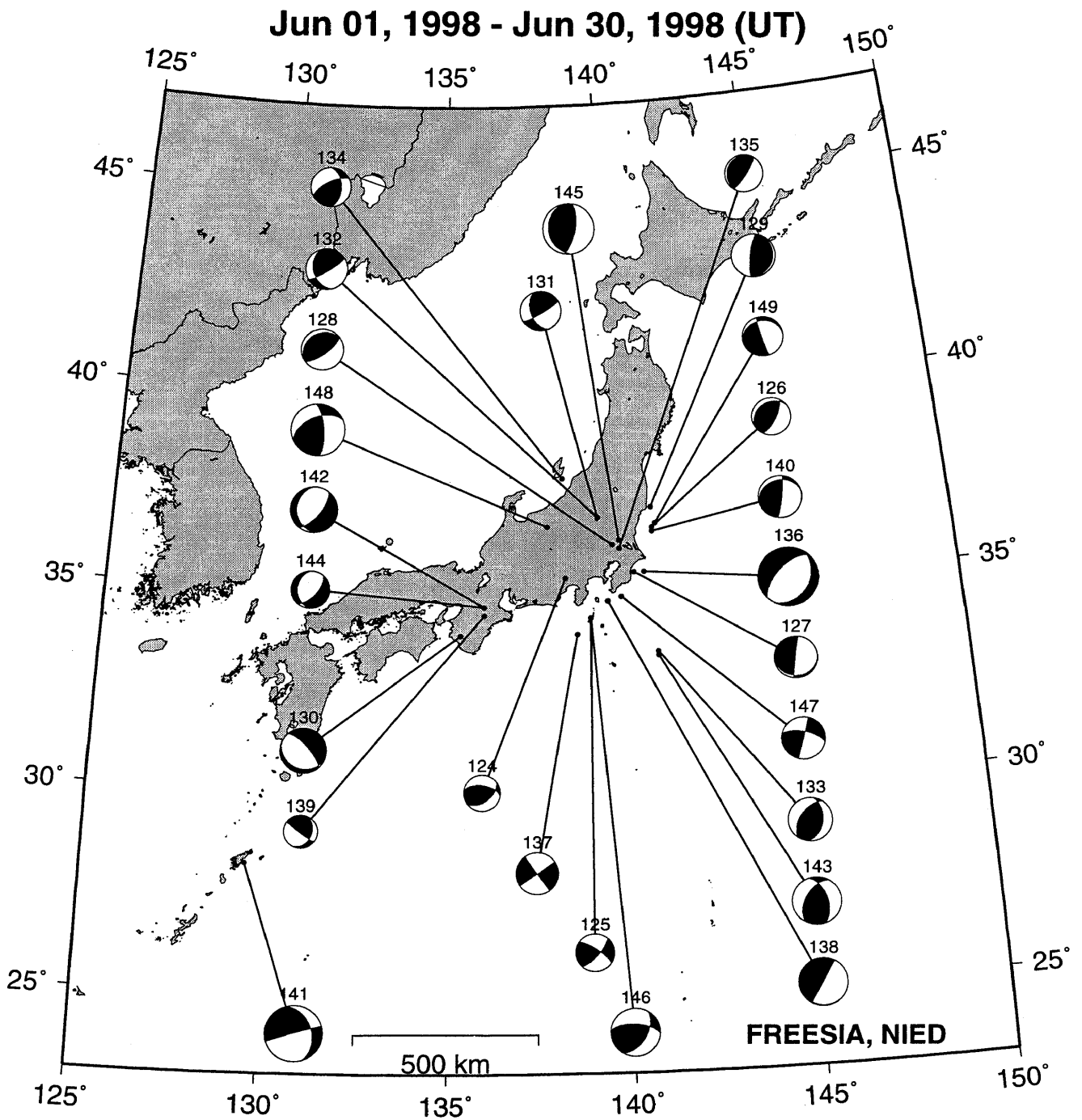


Fig. 2 Estimated focal mechanisms plotted with epicentral locations (continued).

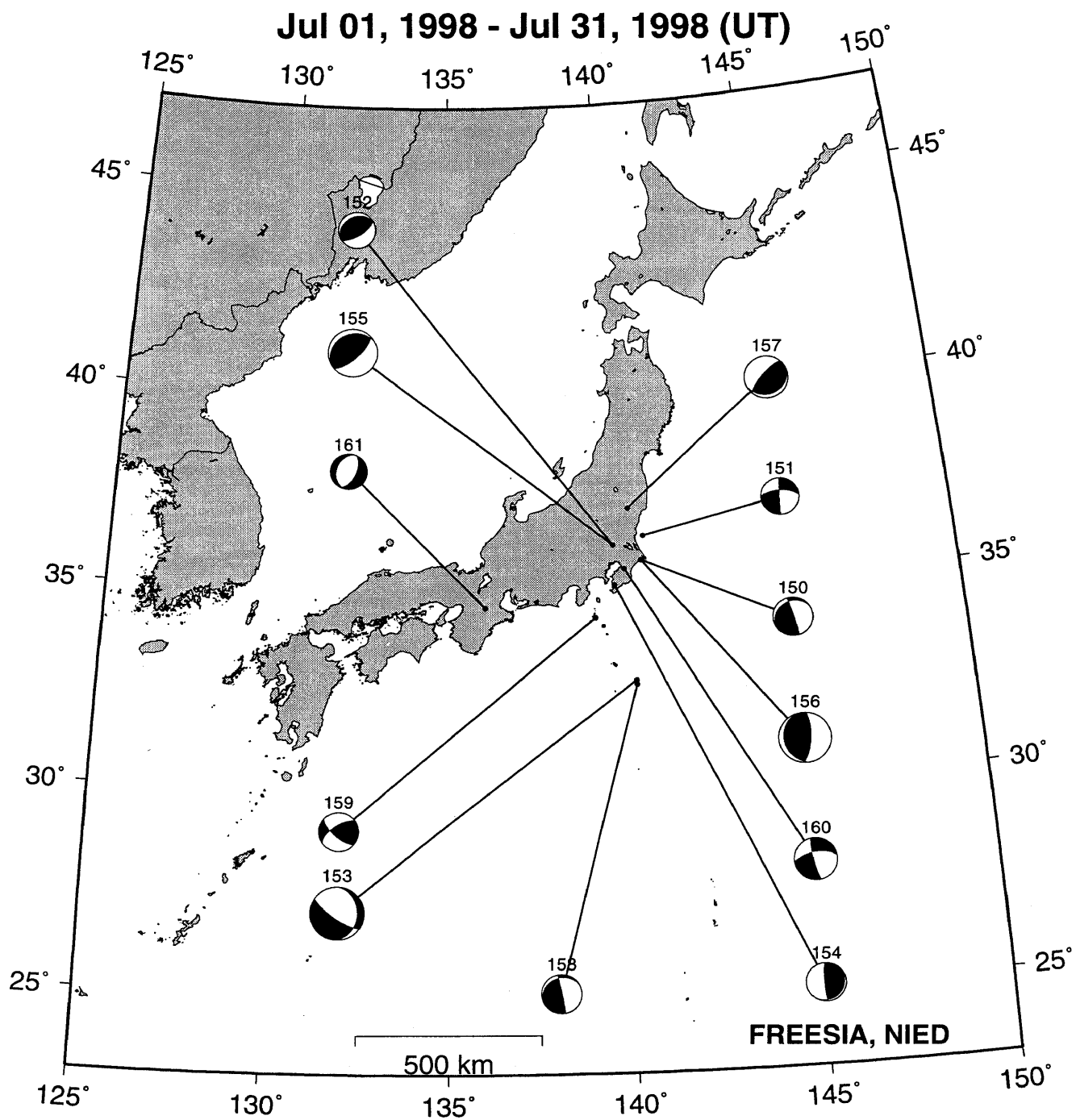


Fig. 2 Estimated focal mechanisms plotted with epicentral locations (continued).

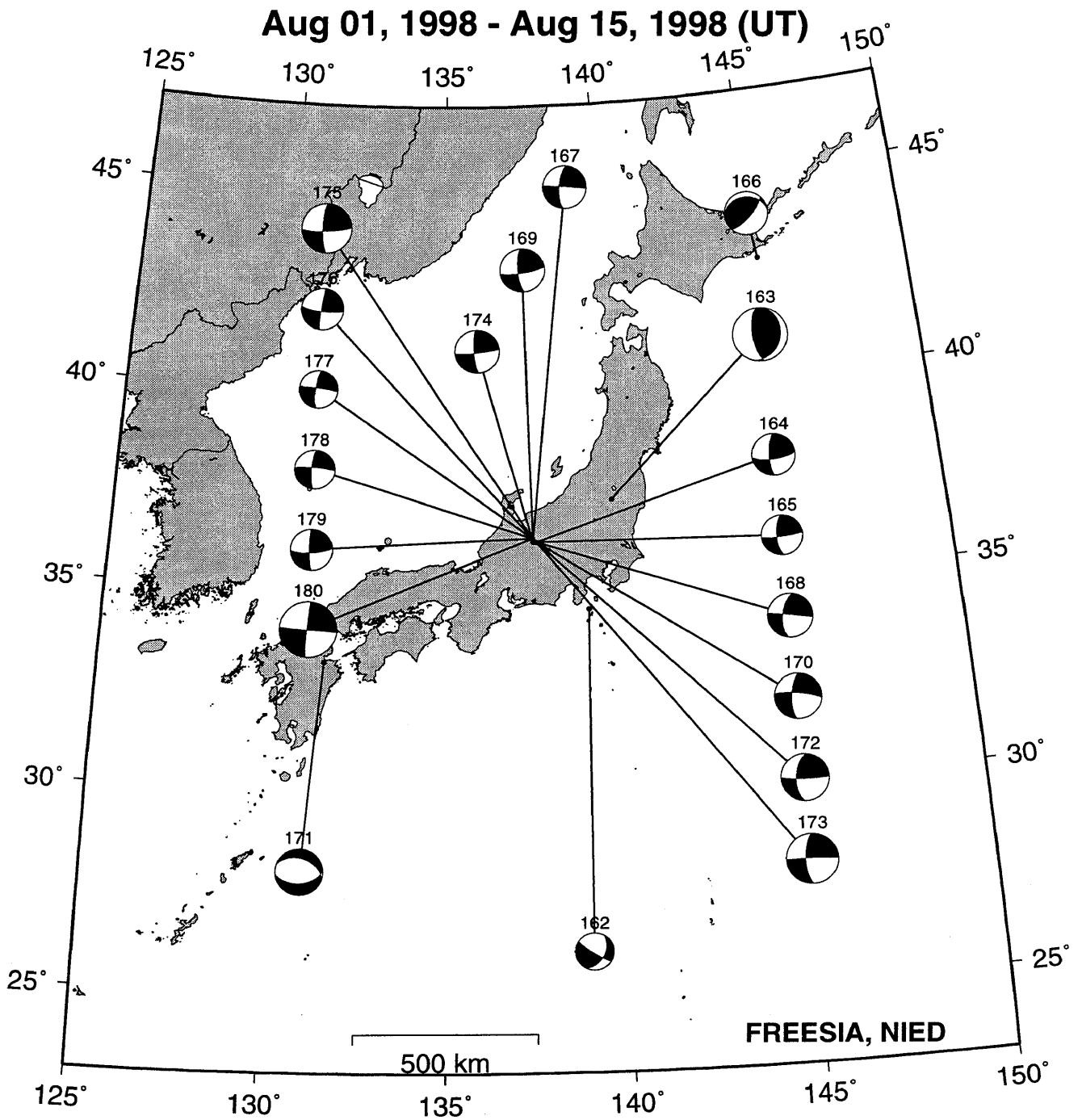


Fig. 2 Estimated focal mechanisms plotted with epicentral locations (continued).

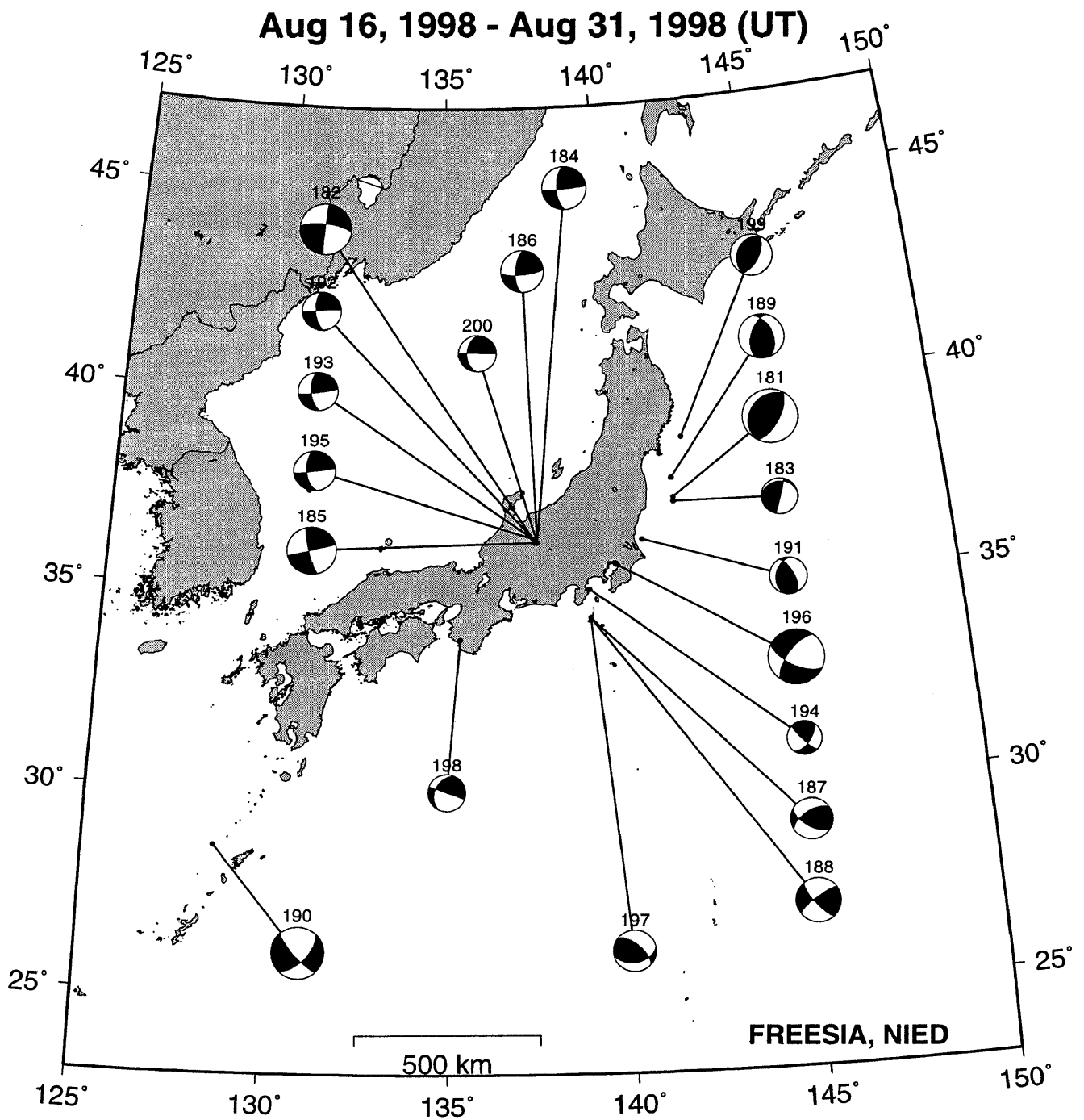


Fig. 2 Estimated focal mechanisms plotted with epicentral locations (continued).

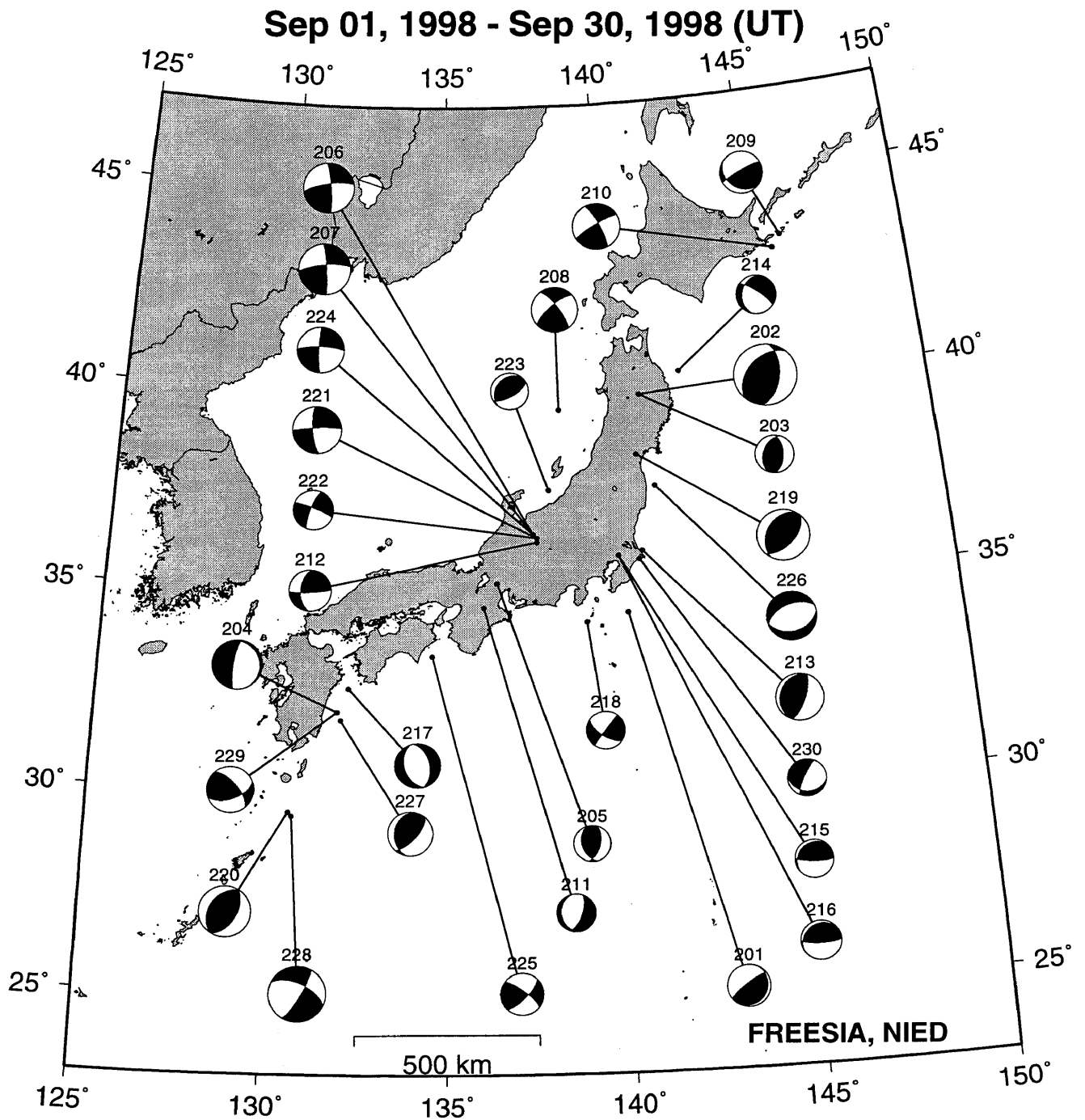


Fig. 2 Estimated focal mechanisms plotted with epicentral locations (continued).

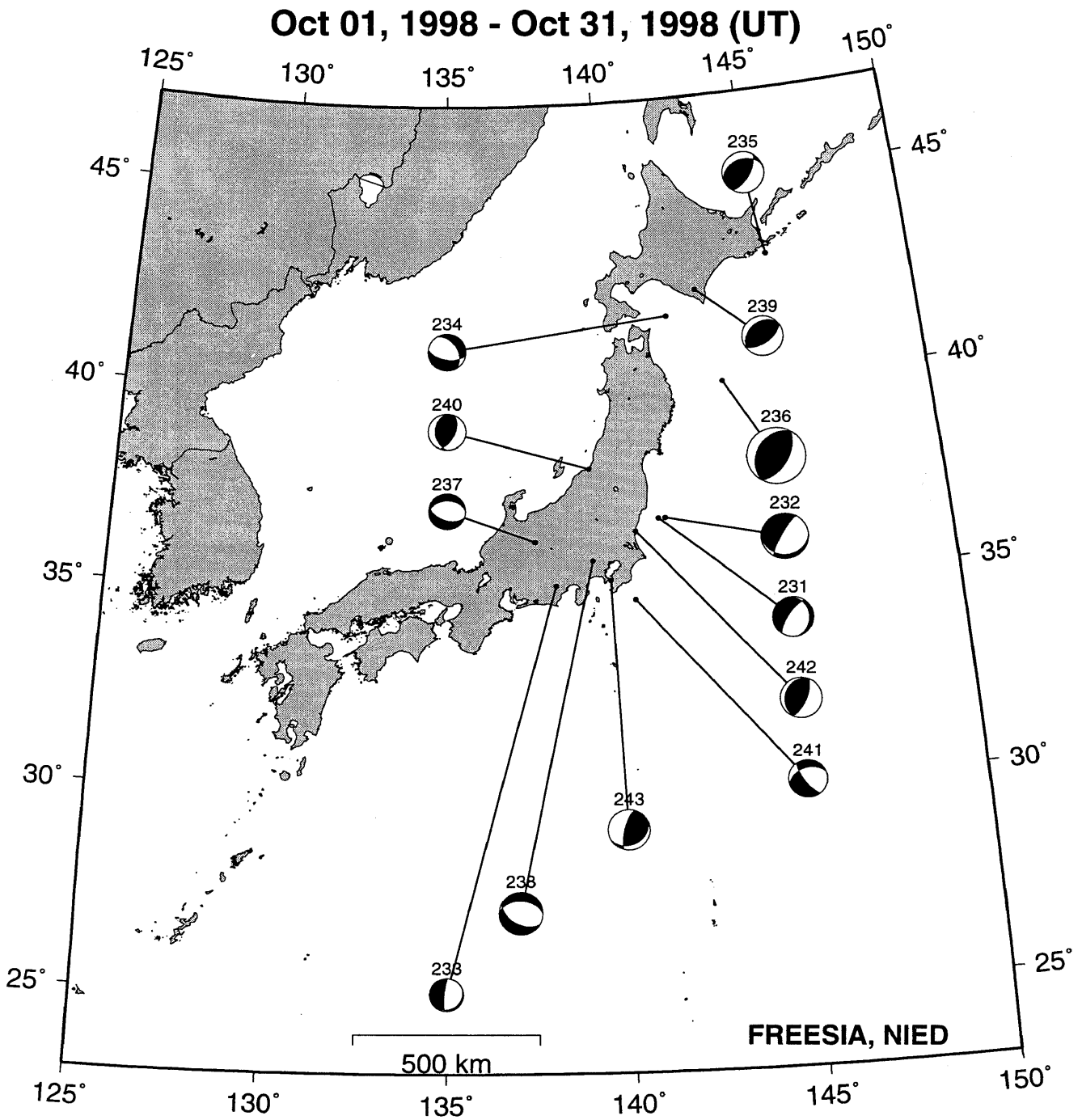


Fig. 2 Estimated focal mechanisms plotted with epicentral locations (continued).

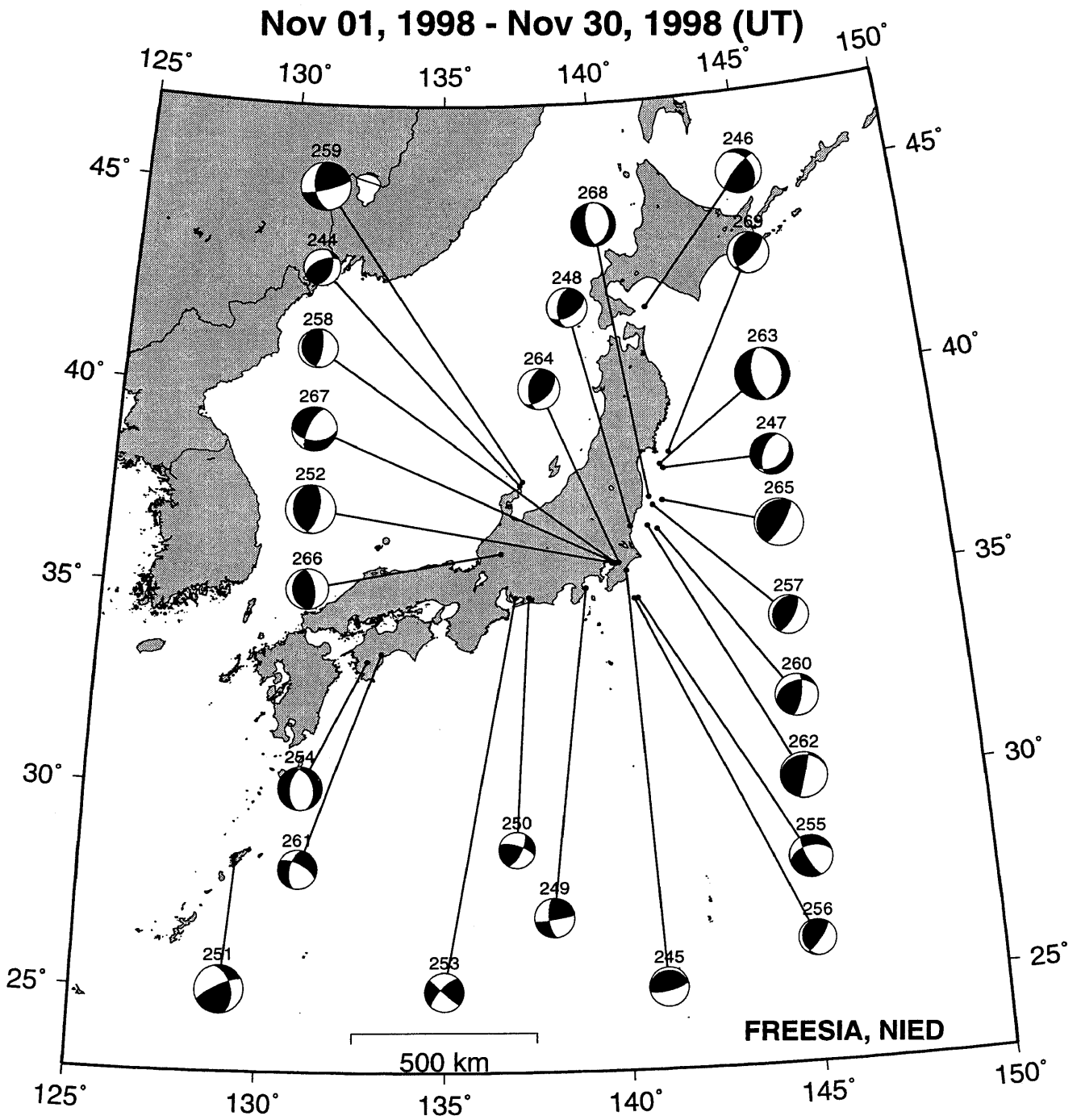


Fig. 2 Estimated focal mechanisms plotted with epicentral locations (continued).

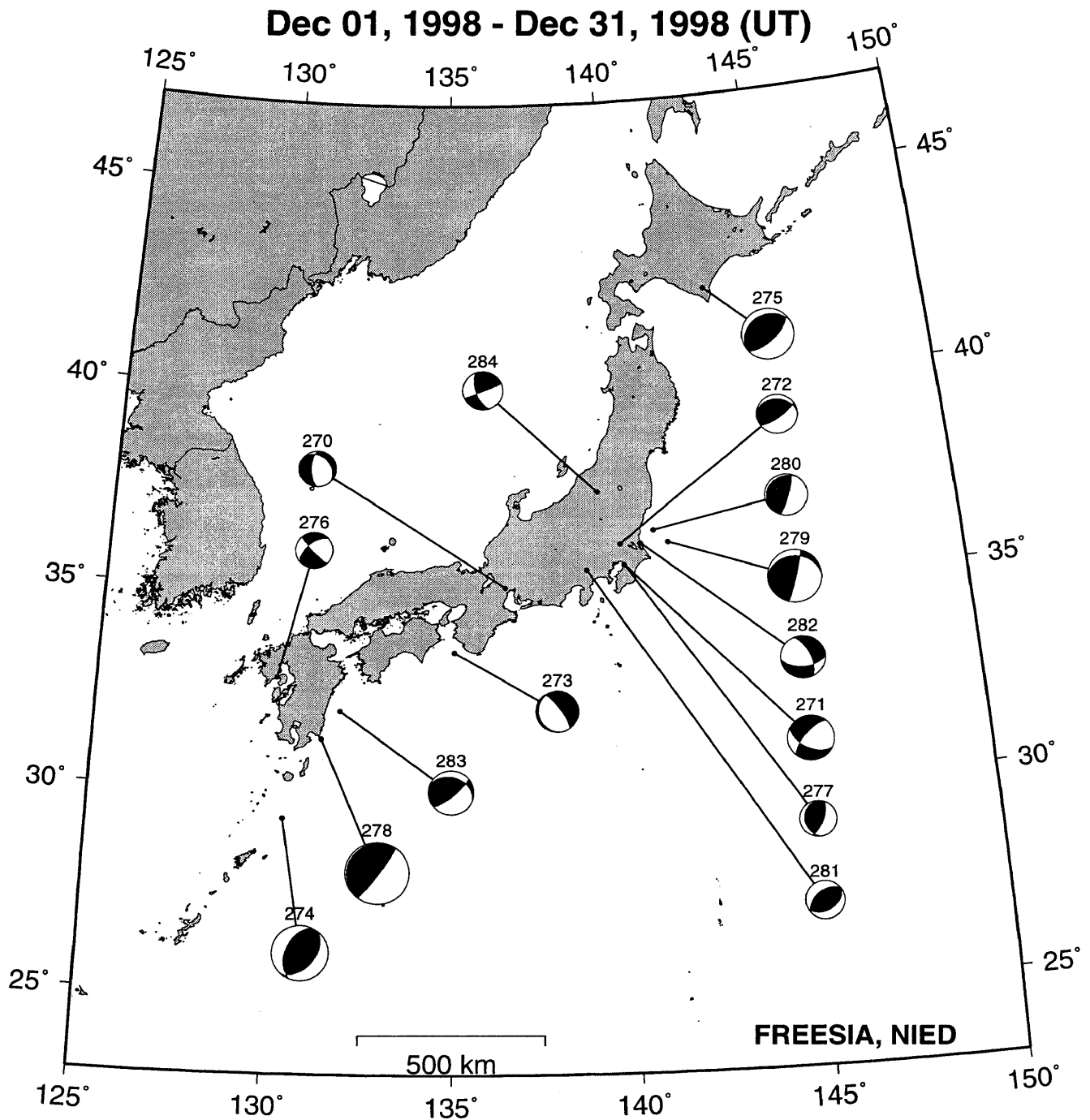


Fig. 2 Estimated focal mechanisms plotted with epicentral locations (continued).

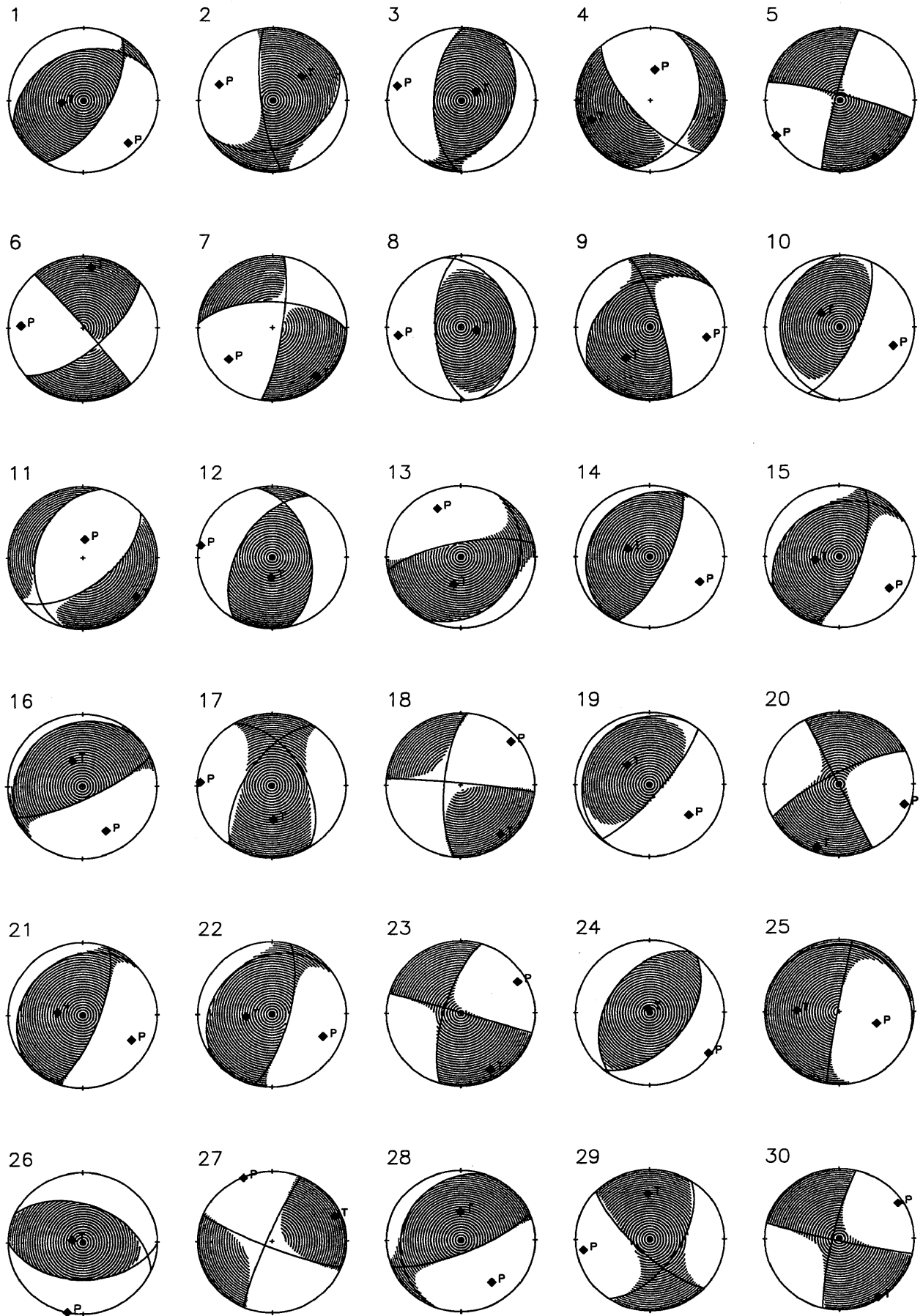


Fig. 3 Estimated moment tensors plotted to the lower hemisphere. P- and T-axes are also plotted.

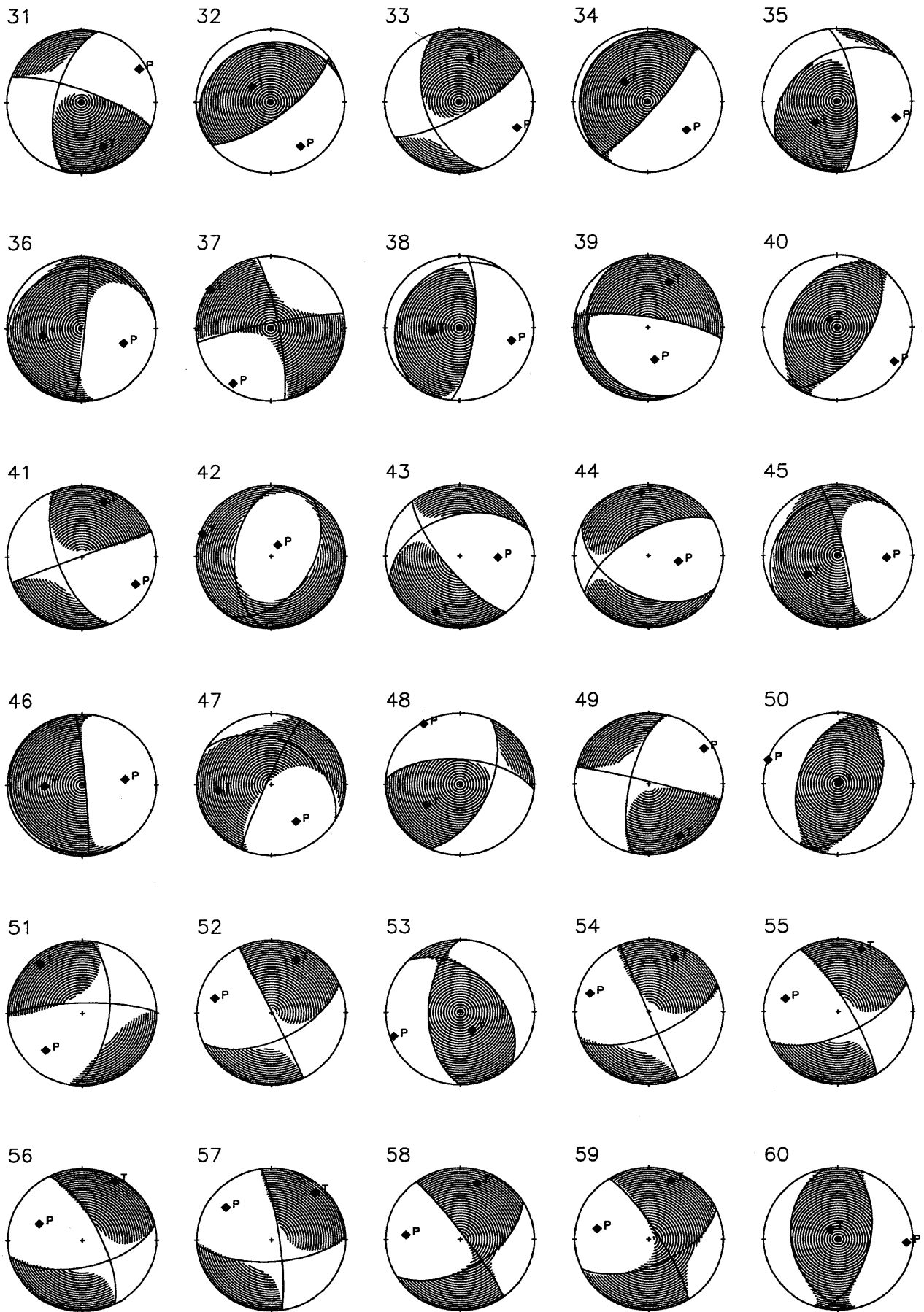


Fig. 3 Estimated moment tensors plotted to the lower hemisphere (continued).

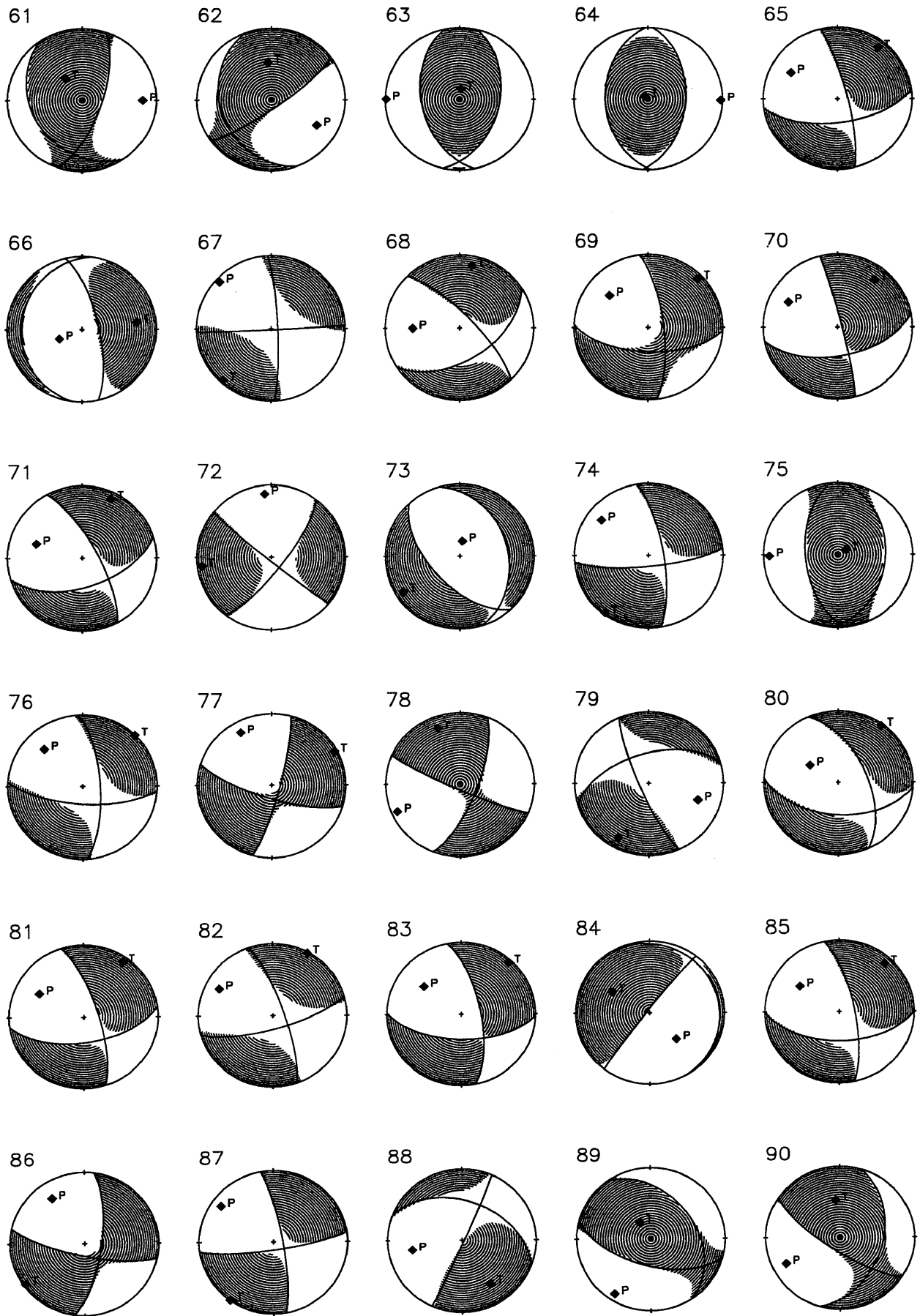


Fig. 3 Estimated moment tensors plotted to the lower hemisphere (continued).

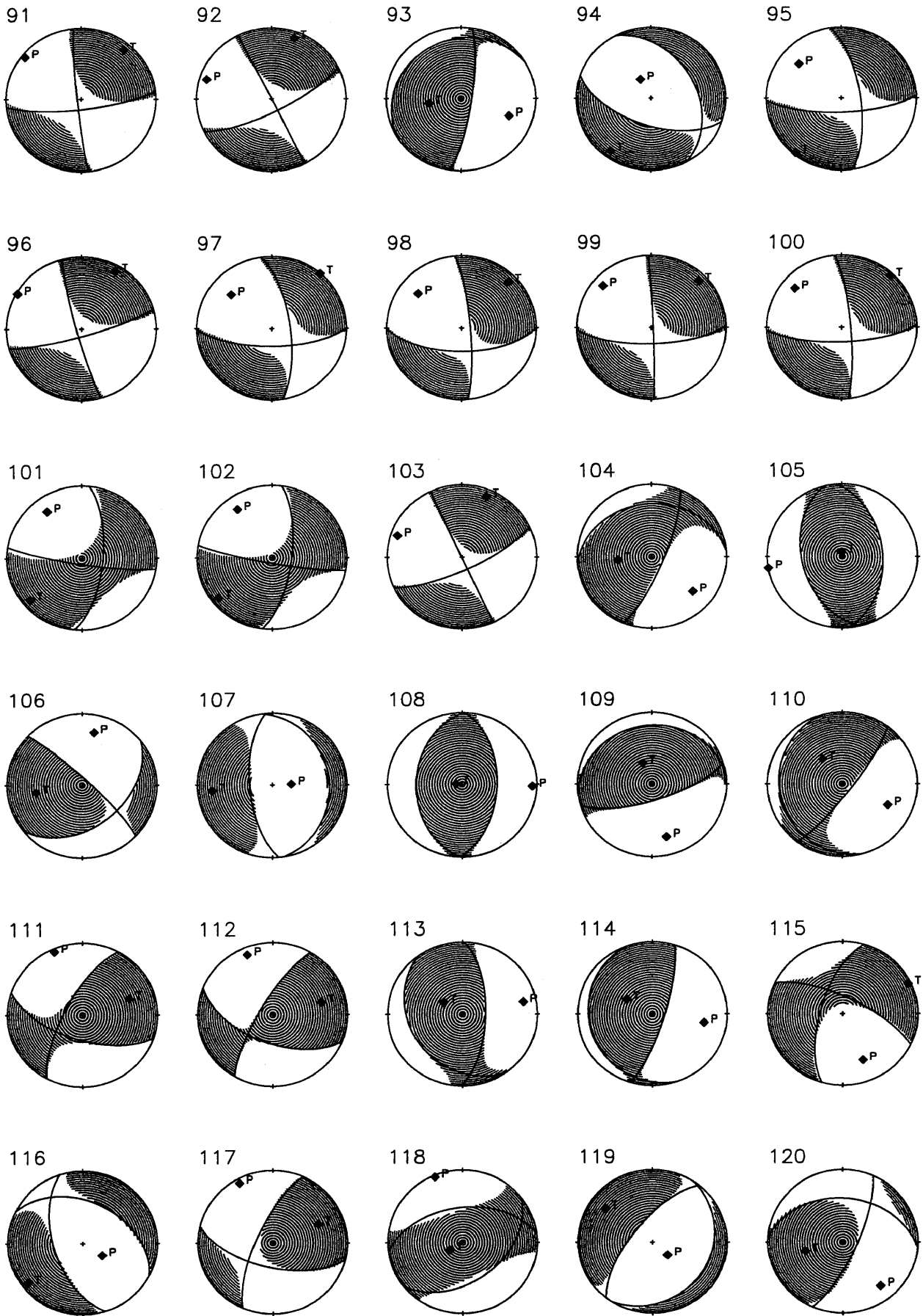


Fig. 3 Estimated moment tensors plotted to the lower hemisphere (continued).

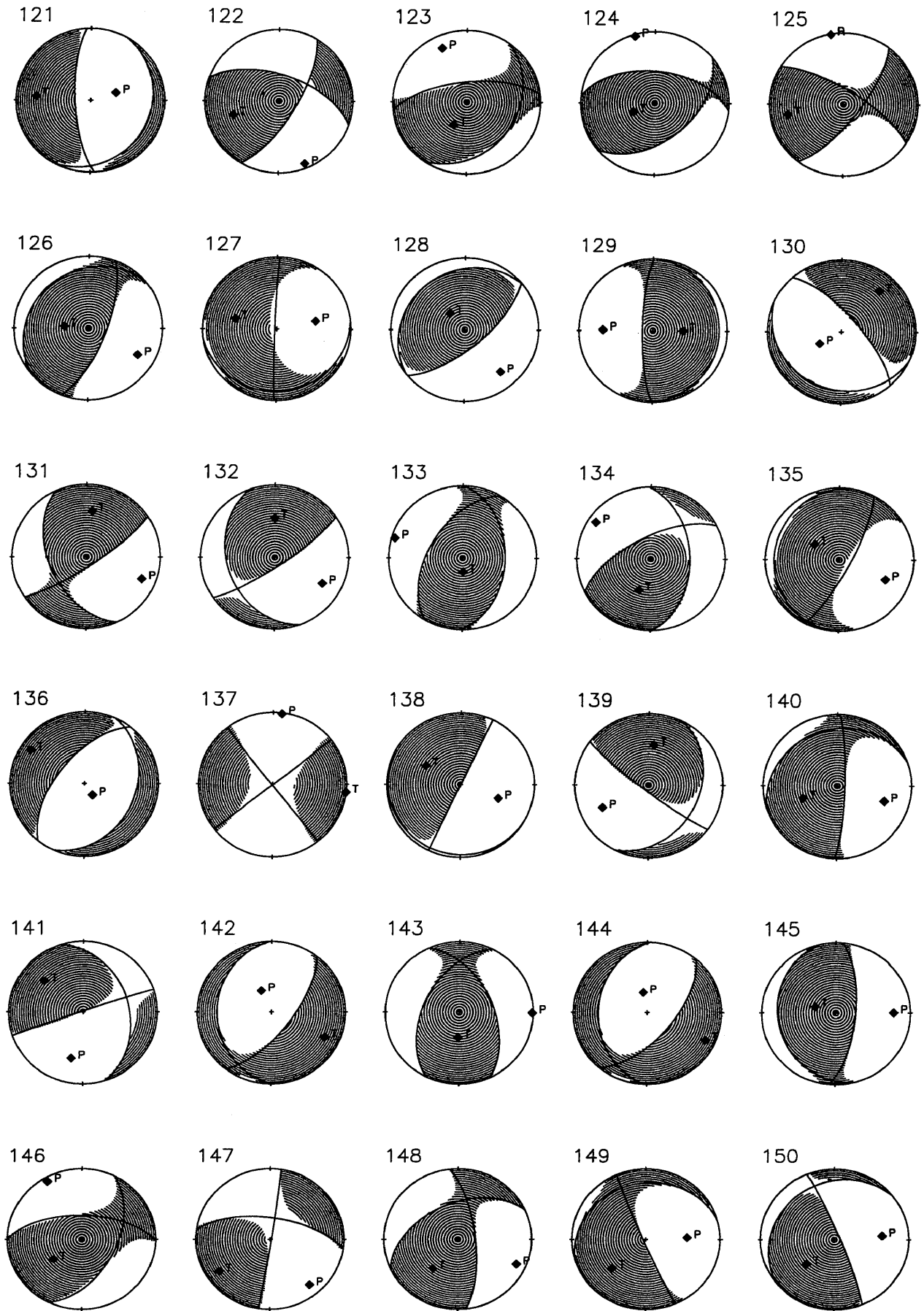


Fig. 3 Estimated moment tensors plotted to the lower hemisphere (continued).

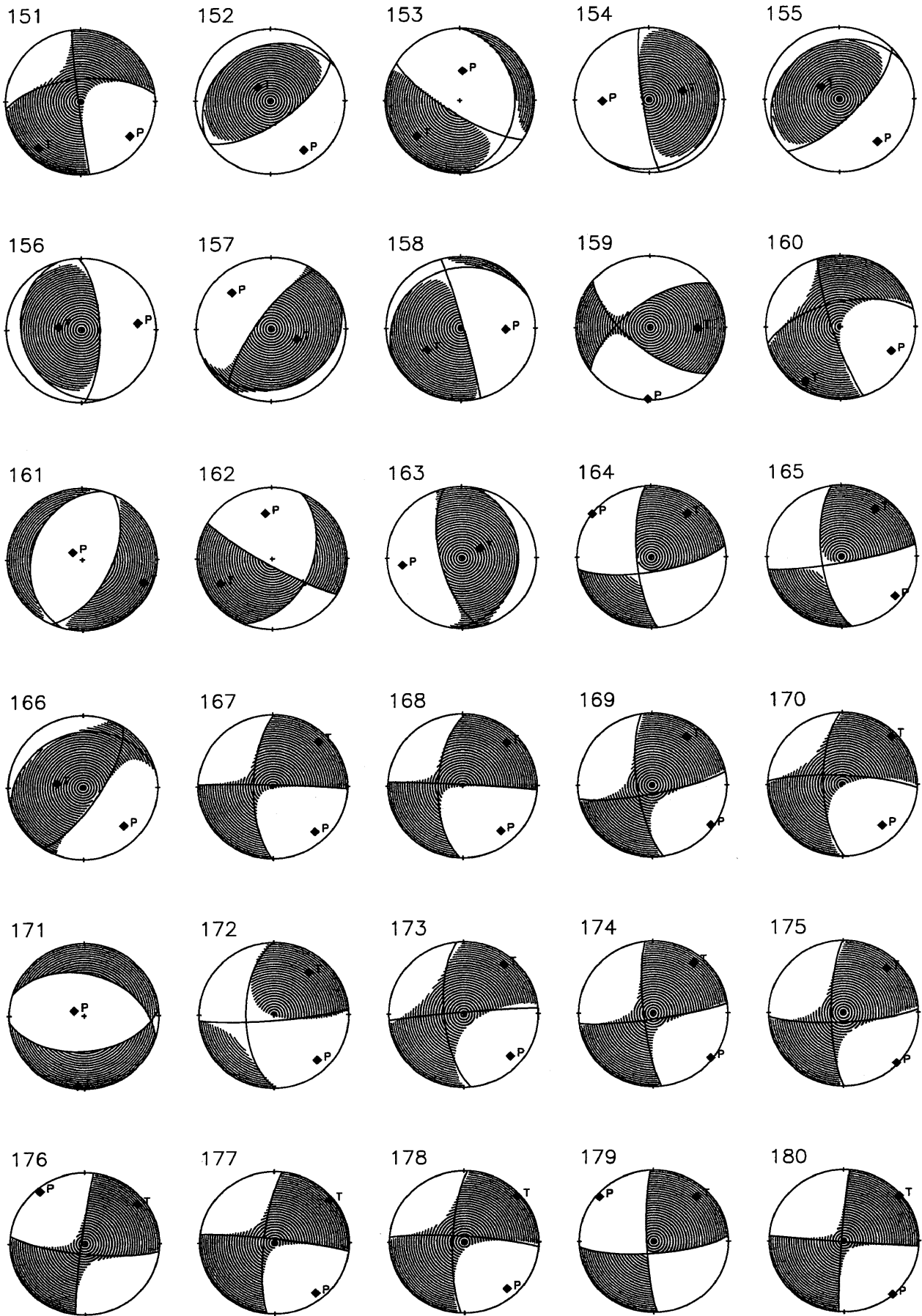


Fig. 3 Estimated moment tensors plotted to the lower hemisphere (continued).

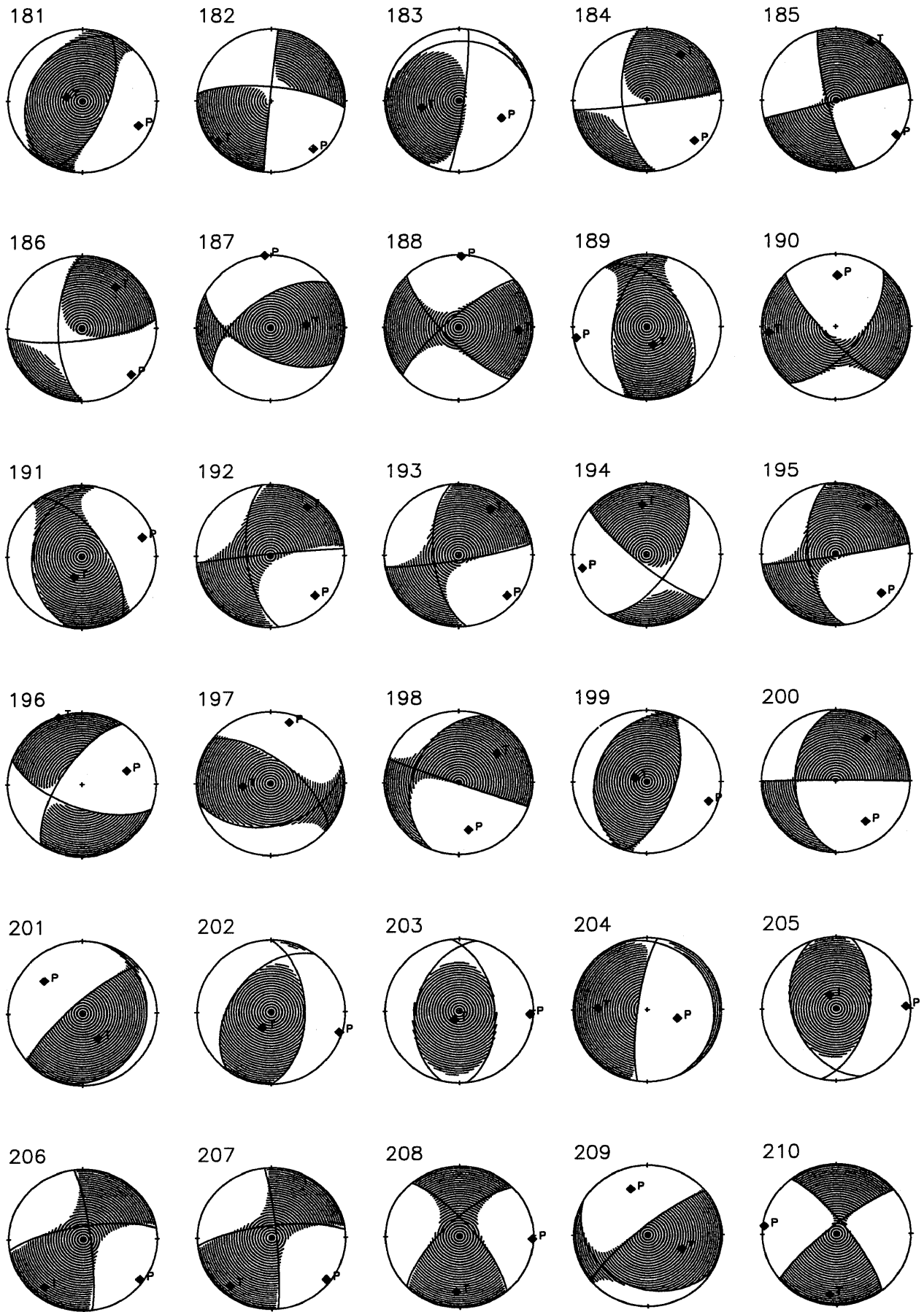


Fig. 3 Estimated moment tensors plotted to the lower hemisphere (continued).

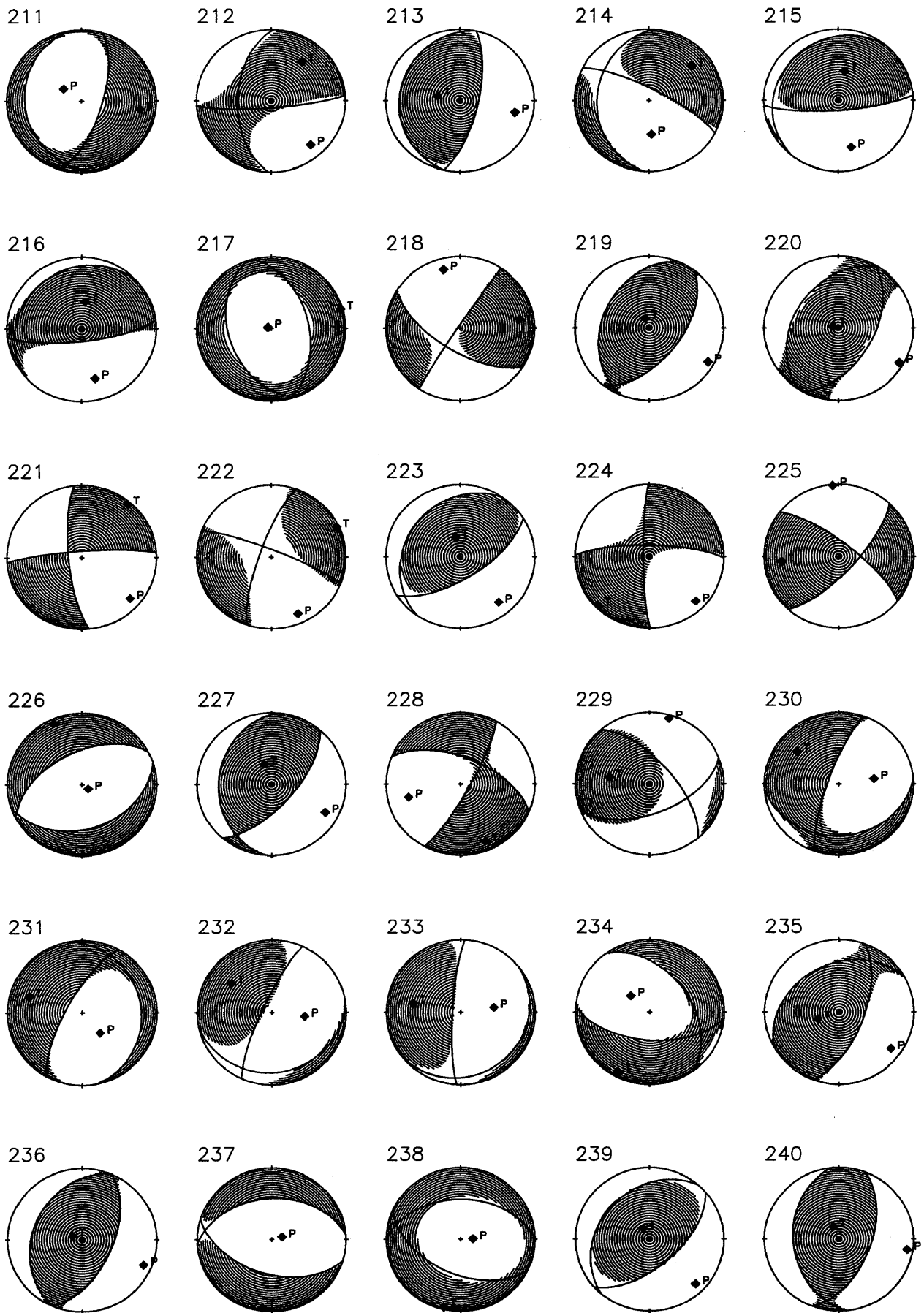


Fig. 3 Estimated moment tensors plotted to the lower hemisphere (continued).

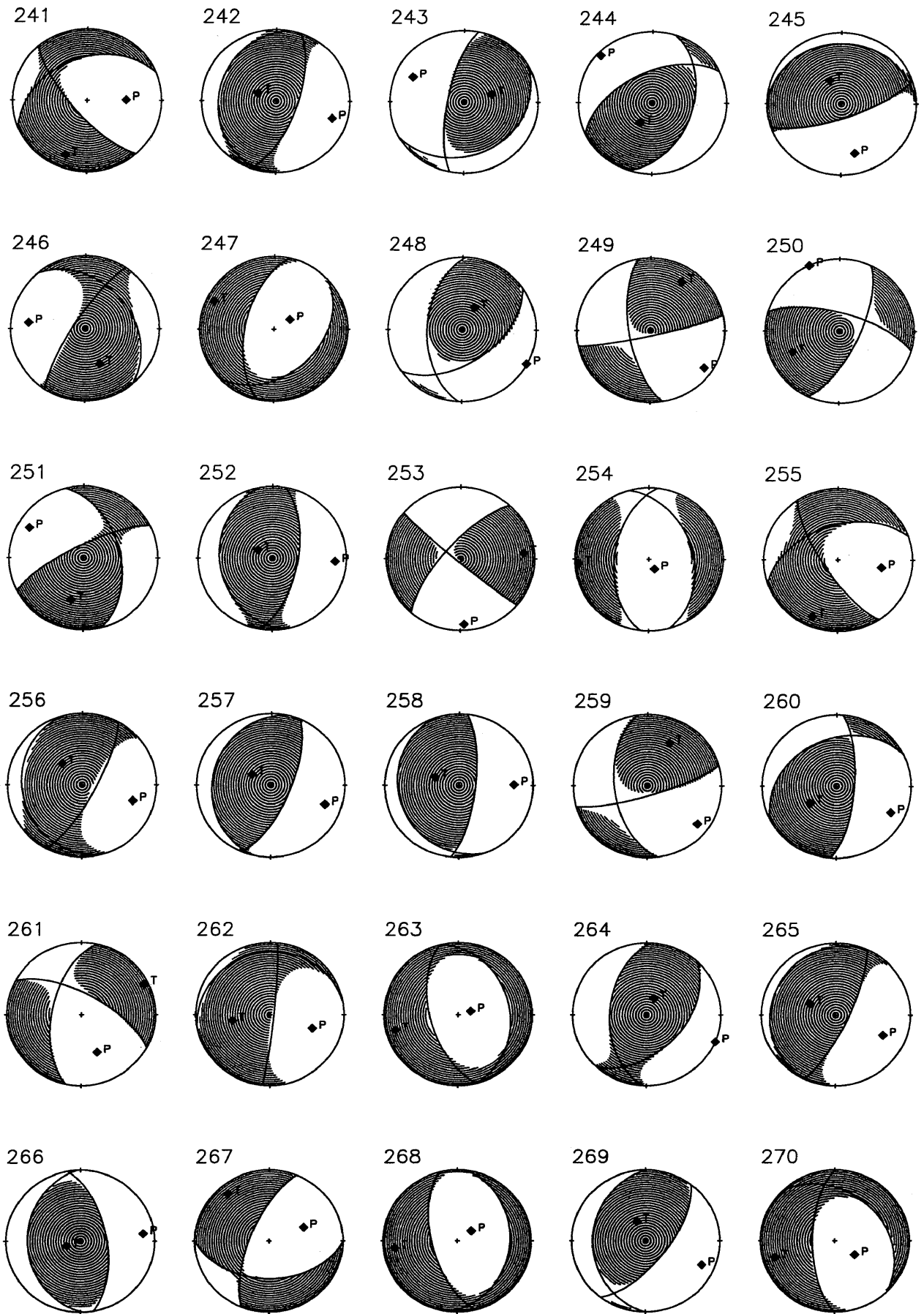


Fig. 3 Estimated moment tensors plotted to the lower hemisphere (continued).

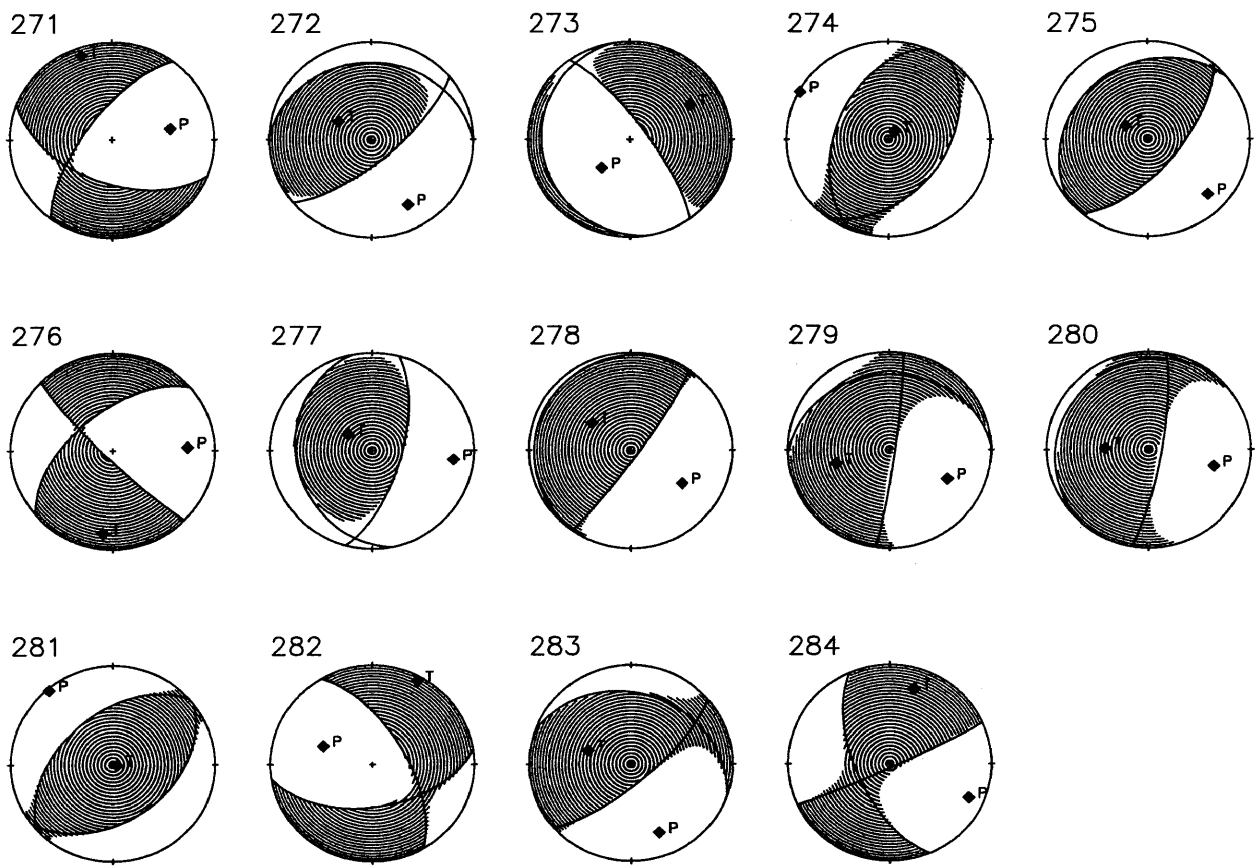


Fig. 3 Estimated moment tensors plotted to the lower hemisphere (continued).